

Phonon-mediated repulsion, sharp transitions and (quasi)self-trapping in the extended Peierls-Hubbard model

J. Sous,^{1,2,*} M. Chakraborty,³ C. P. J. Adolphs,^{1,2} R. V. Krems,⁴ and M. Berciu^{1,2}

¹*Department of Physics and Astronomy, University of British Columbia, Vancouver, British Columbia, Canada, V6T 1Z1*

²*Stewart Blusson Quantum Matter Institute, University of British Columbia, Vancouver, British Columbia, Canada, V6T 1Z4*

³*Department of Physics, Indian Institute of Technology, Kharagpur, India*

⁴*Department of Chemistry, University of British Columbia, Vancouver, British Columbia, Canada, V6T 1Z1*

(Dated: January 3, 2018)

We study two identical fermions, or two hard-core bosons, in an infinite chain and coupled to phonons by interactions that modulate their hopping as described by the Peierls/Su-Schrieffer-Heeger (SSH) model. We show that exchange of phonons generates effective nearest-neighbor *repulsion* between particles and also gives rise to interactions that move the pair as a whole. The two-polaron phase diagram exhibits two sharp transitions, leading to light dimers at strong coupling and the flattening of the dimer dispersion at some critical values of the parameters. This dimer (quasi)self-trapping occurs at coupling strengths where single polarons are mobile. This illustrates that, depending on the strength of the phonon-mediated interactions, the coupling to phonons may completely suppress or strongly enhance quantum transport of correlated particles.

Introduction: Strongly correlated quantum materials exhibit rich physics with many features yet to be understood. Correlated lattice systems are modeled by the extended Hubbard model, which includes inter-site interactions giving rise to interesting physics such as superfluid - Mott insulator transitions [1], antiferromagnetism [2, 3], high-Tc superconductivity [4], twisted superfluidity [5], supersolids [6]. However, the extended Hubbard model does not include interactions with phonons, which are essential for quantum materials. Here, we show that the interplay of the extended Hubbard interactions with phonon-mediated couplings leads to new unique features, such as self-trapping of correlated pairs and the formation of light (mobile) dimers in the regime of strong interactions, both between the particles and with phonons.

A particle (electron, exciton, etc.) dressed with phonons is a polaron. If phonons modulate the on-site energy of the particle, as is the case for electrons in ionic lattices, polarons can be viewed as the bare particle dragging a cloud of phonons. Such polarons are always heavier than the bare particle [7–15]. On the other hand, phonons also modulate the hopping of the particle between sites. Such interactions are important for electrons in conjugated polyenes, where they are described by the Su-Schrieffer-Heeger (SSH) model [16–20], or for excitons in molecular solids, where they are described by the Peierls model. Polarons arising from the SSH/Peierls interactions exhibit sharp transitions [21] into strong-coupling regimes where the polaron (dressed particle) is *lighter* than the bare particle [21–26].

The interplay of the SSH/Peierls couplings and the extended Hubbard interactions may alter the behaviour of strongly correlated quantum systems. For example, in the limit of half-filling, an interplay of phonon-mediated attraction with repulsive Hubbard interactions is known

to lead to a competition between the Mott-insulator and Peierls-insulator phases [27]. Here, we consider polarons arising in the two-particle limit of an extended Hubbard model coupled to phonons through the SSH/Peierls couplings. This is critical for understanding quantum transport of interacting excitons in devices based on organic semiconductors (such as low-temperature solar cells) [28, 29] and the prospects of observing the Mott-insulator/Peierls-insulator competition with highly controllable ultracold atoms/molecules systems, which require understanding of emergent interactions in the few-particle limit. The extended Peierls-Hubbard model can be realized for hard-core bosons with ions in rf-traps [30–33], Rydberg atoms exchanging excitations [34–38], self-assembled ultracold dipolar crystals [39–41], arrays of polar molecules trapped in optical lattices [42, 43], arrays of superconducting qubits [44–49], and J-aggregates [50]. Similar physics may also arise in the context of interacting impurities in a Fermi degenerate gas [51–53] or Bose-Einstein condensates [54–59] of ultracold atoms. Motivated by these experiments, we consider identical fermions/hard-core bosons and show that the interplay between particle statistics, particle interactions and coupling to phonons leads to unique features such as *phonon-mediated repulsion* and *sharp transitions* in the ground-state properties of dimers including one suggestive of *self-trapping*.

Model: We consider two identical fermions (fermionic atoms in the same internal state), or equivalently, two hard-core bosons, placed in an infinite chain [60, 61] described by the Hamiltonian $\mathcal{H} = \mathcal{H}_p + \mathcal{H}_{ph} + \hat{V}$, where:

$$\mathcal{H}_p = -t \sum_i \left(c_i^\dagger c_{i+1} + h.c. \right) + U \sum_i \hat{n}_i \hat{n}_{i+1} \quad (1)$$

is the extended Hubbard model of the bare particles with infinite on-site repulsion, $\mathcal{H}_{ph} = \Omega \sum_i b_i^\dagger b_i$ is the phonon

*Correspondence to jsous@physics.ubc.ca

Hamiltonian (in units of $\hbar = 1$), and

$$\hat{V} = g \sum_i \left(c_i^\dagger c_{i+1} + h.c. \right) \left(b_i^\dagger + b_i - b_{i+1}^\dagger - b_{i+1} \right) \quad (2)$$

is the Peierls/SSH particle - phonon coupling [21]. Here, i is the site index, $\hat{n}_i = c_i^\dagger c_i$, U is the strength of the bare nearest-neighbor (NN) interactions and Ω is the phonon frequency. We characterize the particle - phonon effective coupling by the dimensionless parameter $\lambda = 2g^2/(\Omega t)$.

Methods: We use two methods to investigate this problem. The first is variational exact diagonalization (VED), a well-established, unbiased numerical method, where the variational basis set is expanded systematically, starting from the Bloch state for two adjacent particles and zero phonons [62–64]. The second method is based on the Momentum Average (MA) approximation, a quasi-analytical variational method that has been shown to be accurate for polarons [65–67], including SSH polarons [21]. Here, we generalize MA to study bound dimers by allowing a variational space where the two particles are either in adjacent sites or two sites apart, interacting with a phonon cloud spread over at most three adjacent sites (for more details, see the Supplementary Information); we comment more on these choices below.

Results: First, we set $U = 0$ and study whether exchange of phonons suffices to bind two SSH polarons into a bipolaron. For reference, we note that equivalent 1D models with long(er)-range on-site energy-modulating couplings, such as the screened and unscreened Fröhlich couplings, show the appearance of stable bipolarons; for on-site Holstein coupling, such bipolarons do not form [63, 64, 68].

We find that for $U = 0$, bipolarons do not form for any coupling λ . To understand the implications of this result, note that the bare particles ($\lambda = 0$) bind only for $U \leq -2t$. This attraction is needed to compensate for the loss of kinetic energy [69]. The SSH polaron dispersion – and hence its kinetic energy – remains significant at all particle - phonon couplings. Our results thus show that the phonon-mediated interaction is insufficient to compensate for the kinetic energy that would be lost upon binding.

To characterize quantitatively this phonon-mediated interaction, we compute the values of $U = U_C(\lambda)$ corresponding to the onset of stable bound state (we define the bound dimer to be stable if its ground state energy is below the two-polaron continuum). We then compare $U_C(\lambda)$ with $\bar{U}_C(\lambda)$, defined as the NN attraction needed to bind two hard-core particles with dispersions identical to those of single SSH polarons. This latter model mimics the renormalization of the dispersion due to each particle creating and interacting with its own cloud of phonons, but excludes the effective interactions due to phonon exchange between the clouds. The phonon exchange occurs in the full model, so $|\bar{U}_C(\lambda)| - |U_C(\lambda)|$ is an estimate of the phonon-mediated NN attraction between polarons. Figure 1 shows that $|U_C(\lambda)| > |\bar{U}_C(\lambda)|$

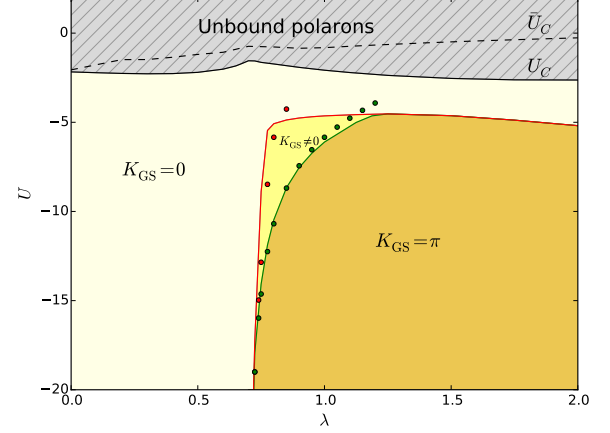


FIG. 1: (color online) Two-polaron phase diagram at $t = 1, \Omega = 3$. The solid black line shows $U_C(\lambda)$ below which stable bound states form, while the dashed line shows $\bar{U}_C(\lambda)$; the difference between the two is the strength of the phonon-mediated interaction. Note that $U_C < \bar{U}_C$, which means that this interaction is repulsive. The red and green lines mark the sharp transitions of the bound dimer's GS. The lines are the VED results and the corresponding symbols are the MA results.

for all λ . This means that the phonon-mediated interaction is in fact *strongly repulsive*, in stark contrast to what is observed for conventional polaron models [63, 64, 68].

This surprising result can be explained by considering the limit $\Omega \gg |t|, |g|$ within perturbation theory (details in Supplementary Information). Projecting out high-energy states with one or more phonons, the effective Hamiltonian for a single polaron becomes

$$\hat{h}_1 = \sum_i \left(-t c_i^\dagger c_{i+1} + t_2 c_i^\dagger c_{i+2} + h.c. \right) - \epsilon_0 \sum_i \hat{n}_i. \quad (3)$$

The small cloud that forms in this limit does not renormalize the NN hopping but it mediates a next-nearest-neighbor (NNN) hopping $t_2 = g^2/\Omega = \lambda t/2$ through the process $c_i^\dagger|0\rangle \xrightarrow{\hat{V}} c_{i+1}^\dagger b_{i+1}^\dagger|0\rangle \xrightarrow{\hat{V}} c_{i+2}^\dagger|0\rangle$. The four processes $c_i^\dagger|0\rangle \xrightarrow{\hat{V}} c_{i\pm 1}^\dagger b_{i\pm 1}^\dagger|0\rangle \xrightarrow{\hat{V}} c_i^\dagger|0\rangle$ and $c_i^\dagger|0\rangle \xrightarrow{\hat{V}} c_{i\pm 1}^\dagger b_i^\dagger|0\rangle \xrightarrow{\hat{V}} c_i^\dagger|0\rangle$ explain the polaron formation energy $\epsilon_0 = 4g^2/\Omega$ [21]. The resulting polaron dispersion $E_P(k) = -\epsilon_0 - 2t \cos(k) + 2t_2 \cos(2k)$ is dominated by the NNN hopping at large λ ; this explains both the transition, at $\lambda = 1/2$, of the polaron ground state (GS) momentum from $k = 0$ to a finite value that smoothly goes to $k = \pi/2$, and why the polaron remains light at large λ (for more discussion, see Ref. [21]).

Repeating the calculation for two particles, we find the corresponding effective Hamiltonian to be

$$\hat{h}_2 = \hat{h}_1 + \epsilon_0 \sum_i \hat{n}_i \hat{n}_{i+1}, \quad (4)$$

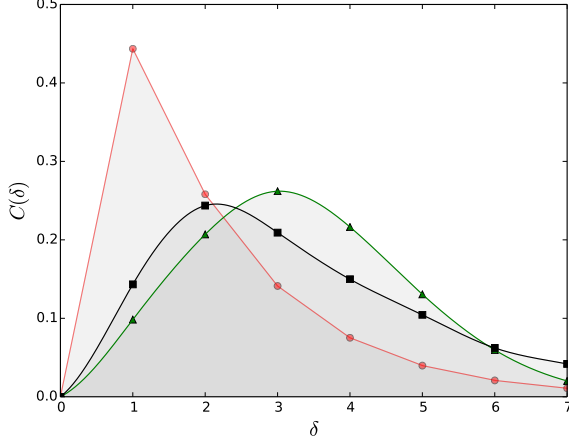


FIG. 2: (color online) Correlation between the two particles $C(\delta) = \langle \Psi_{GS} | \frac{1}{N} \sum_i \hat{n}_i \hat{n}_{i+\delta} | \Psi_{GS} \rangle$ vs separation δ for $U = U_C(\lambda) - 0.5$, $t = 1$, $\Omega = 3$ and $\lambda = 0.1$ (red circles), $\lambda = 0.7$ (green triangles), $\lambda = 2.0$ (black squares).

illustrating the appearance of phonon-mediated NN repulsion. Its origin can be explained as follows: if the polarons are $\delta \geq 2$ sites apart, each lowers its energy by ϵ_0 through hops to its adjacent sites and back, accompanied by virtual phonon emission and absorption, as explained above. However, if the polarons are on adjacent sites, then Fermi statistics blocks half of these processes, *i.e.* each particle can only lower its energy by $\epsilon_0/2$. The energy cost for polarons to be adjacent is, thus, $\epsilon_0 = 2\lambda t$.

It is very important to note that \hat{h}_2 also includes terms such as $c_i^\dagger c_{i+1}^\dagger |0\rangle \xrightarrow{\hat{h}_2} c_{i+1}^\dagger c_{i+2}^\dagger |0\rangle$. However, NNN hopping of one particle past the other is forbidden by statistics (the particle at i cannot emit a phonon and move to $i+1$ because that site is occupied). Instead, these terms describe both particles moving through $c_i^\dagger c_{i+1}^\dagger |0\rangle \xrightarrow{\hat{V}} c_i^\dagger b_{i+1}^\dagger c_{i+2}^\dagger |0\rangle \xrightarrow{\hat{V}} c_{i+1}^\dagger c_{i+2}^\dagger |0\rangle$. In other words, instead of one particle hopping over the other, which is forbidden, each particle moves by one site and a phonon is exchanged in the process. Thus, this term is also a phonon-mediated effective interaction which would be absent if phonons could not be exchanged between particles. In the large Ω limit it happens to precisely compensate for the NNN hopping forbidden by the particles' statistics, but that is not likely to be the case throughout the parameter space. This shows that the functional form of the effective phonon-mediated interaction must also contain such “pair-hopping” terms in addition to the NN repulsion. Such terms do not appear in models where phonons modulate the on-site particle energy (e.g., Holstein and Fröhlich models).

For smaller values of Ω , the phonon clouds have more phonons and are more extended spatially, and thus can mediate longer-range effective interactions and hopping.

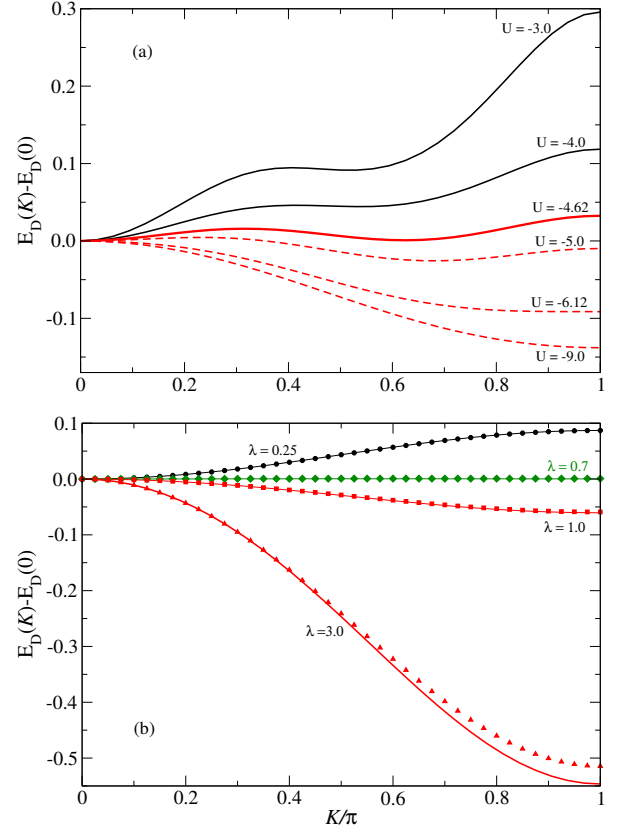


FIG. 3: (color online) Dimer dispersion $E_D(K) - E_D(0)$ for (a) $\lambda = 1$ and various values of U ; and (b) $U = -30$ and various values of λ . In both cases $t = 1$, $\Omega = 3$. The lines are the VED results and the symbols are the MA results. Note the sharp transitions of the GS momentum from $K_{GS} = 0$ to $K_{GS} > 0$ in both cases.

Indeed, as shown in Fig. 2 for $\Omega = 3$ and $U = U_C(\lambda) - 0.5$, *i.e.* just inside the dimer stability region, the bound particles favor adjacent locations only for $\lambda \rightarrow 0$. At moderate and strong couplings they are found with highest probability to be 2 or even 3 sites apart, even though the bare attraction is NN only. This suggests that the strong phonon-mediated NN repulsion is supplemented by longer range effective attraction, and/or that binding is due to kinetic energy gained through phonon-mediated “pair-hopping” terms such as the one discussed above.

We now examine the properties of dimers formed when U is sufficiently large to balance the phonon-mediated repulsion and the loss of kinetic energy. Figure 3 shows the dimer dispersion, $E_D(K)$ as a function of U and λ , illustrating two unique features of dimers arising from the SSH coupling. At low $|U|$ and/or λ , the dimer ground state has momentum $K_{GS} = 0$. As λ and/or $|U|$ increases, there is a sharp transition to a GS momentum $K > 0$. Fig. 3(a) shows that with increasing $|U|$, the dimer dispersion develops a rather unusual shape with a second local minimum appearing at a finite momentum. At $U \approx -4.62t$ this minimum becomes degenerate with that at $K = 0$, and the dimer ground-state momentum

jumps discontinuously to $K_{GS} \approx 0.6\pi$ and then continues to increase with increasing $|U|$. There is a second sharp transition to $K_{GS} = \pi$ at $U = -6.12t$. These curves are at a fixed λ so the polaron dispersion is unchanged. The change in the dimer dispersion (and in K_{GS}) is therefore due to forcing the bound polarons closer, as $|U|$ increases.

In Fig. 3b we follow the evolution of $E_D(K)$ with λ for a fixed $U = -30t$. At small λ we see a rather heavy dimer with $K_{GS} = 0$, as expected because in this limit the non-interacting polarons are quite heavy and with $E_P(k)$ increasing monotonically with k [21]. With increasing λ the effective dimer mass increases fast and the dispersion becomes flat. At a value $\lambda^* \approx 0.7$ the minimum jumps discontinuously to $K_{GS} = \pi$. It stays there with further increase in λ , but the bandwidth increases dramatically as the phonon-mediated pair-hopping terms become dominant, thus making the dimers light at strong coupling.

Figure 1 illustrates the locations of these sharp transitions for the dimers in the extended Peierls-Hubbard model on the U - λ phase diagram. To the best of our knowledge, this is the first observation of such sharp transitions of the two-polaron ground state. They never occur in Holstein or Fröhlich models, where the bipolarons always have $K_{GS} = 0$ [63, 64, 68].

The second unique feature illustrated in Figure 3 is the flattening of the dimer dispersion at $\lambda = \lambda^* \approx 0.7$, suggestive of *self-trapping*: here the dimers are essentially localized even though the single polarons have finite bandwidth. This behavior can be understood qualitatively as follows. For small λ , the polaron dispersion is dominated by its NN hopping. A large $|U|$ can bind the polarons only when they are on adjacent sites. When acting on such a configuration, NN hopping moves the particles two sites apart to an energetically expensive configuration. As a result, the effective dimer dispersion acquires a term $\sim -t^2/|U| \cos(K)$, which favors $K_{GS} = 0$ (see Supplementary Information). On the other hand, at finite λ , the “pair-hopping” process moving the NN pair as a whole also becomes active and contributes a term of order $2t_2 \cos(K)$ to the dimer dispersion (see Supplementary Information); this term favors $K_{GS} = \pi$. At $\lambda = \lambda^*$ the two terms cancel and the bandwidth collapses. However, numerical simulations cannot guarantee that the bandwidth is precisely zero, and we do not have theoretical arguments why the longer range hopping should also vanish at λ^* . This is why we prefer to use the more conservative term of (quasi) self-trapping.

Before concluding, we highlight another accomplishment of this work, demonstrated by Figs. 1 and 3, namely the successful generalization of the MA approximation to bipolaron-type problems. The variational space we implemented here (see Supplementary Information) is designed, by construction, to describe strongly bound polarons. Indeed, the MA predictions are in quantitative agreement with VED in this limit. The MA results are also qualitatively correct near $U_C(\lambda)$ (not shown), but its accuracy is much poorer for weakly bound po-

larons. A suitable increase of the variational space is necessary to improve the accuracy of the MA approximation for weakly bound states. This can be done in a rather straightforward way and promises to establish MA as an equally valuable and efficient method for the study of bipolarons as it is for polarons.

Discussion: To summarize, we showed that dressing interacting particles by phonons through SSH/Peierls couplings leads to very rich two-polaron physics, qualitatively different from what is known for conventional polaron models. We showed that for bare particles with the statistics of identical fermions or of hard-core bosons, the phonon-mediated interactions are repulsive, contradicting the conventional view that phonons act as “glue” for quasiparticles. We showed that the “pair-hopping” terms, which are also mediated by phonon-exchange and can only arise in models with phonons modulating the particle hopping, play a major role, leading to *sharp transitions* of the bound dimer’s ground state. We also observe the collapse of the dimer’s dispersion at phonon coupling strength λ^* where the single polarons are mobile, suggestive of a self-trapping transition.

As discussed in the previous section, all these new observations rest on the interplay of two generic features: hard-core statistics of bare particles and off-diagonal, hopping-dependent particle-phonon couplings. As such, these results apply to a wide range of systems and have far-reaching implications for complex quantum systems of interacting dressed particles. The Hamiltonians considered here describe the interactions of small excitons coupled to phonons, particularly relevant to molecular crystals and organics semiconductors [28, 29]. Moreover, the hopping-dependent interactions with phonons, such as the one described by Eq. (2), are generally present in all materials. They may not always be dominant but, because they lead to qualitatively distinct behaviour of the resulting dressed particles, our work raises an important question of how the interplay of the coupling terms in Eq. (2) with conventional phonon-induced interactions changes the dynamics of polarons. As we showed in previous work [43], a perturbative admixture of the hopping-dependent interactions may lead to non-perturbative changes of the single polaron dispersion. If a similar effect happens for dimers or bipolarons at experimentally relevant interaction parameters, many of the long-standing questions in polaron physics must be revisited to account for the hopping-dependent interactions with phonons.

In addition, our results suggest that soft-core bosons and/or singlet fermions may form highly mobile bipolarons with sharp transitions even in the limit of vanishing U ; we are currently investigating this. Also, many of these features are expected to apply to systems with more particles. The “pair-hopping” terms must be equally important for few-polaron ensembles, suggesting that the ground state of few-polaron states must also exhibit sharp transitions and, perhaps, localization (self-trapping).

Acknowledgements: This work was supported by NSERC of Canada and the Stewart Blusson Quantum Matter Institute. J. S. acknowledges discussions with Ian Affleck. M. C. appreciates access to the computing facilities of the DST-FIST (phase-II) project installed in the Department of Physics, IIT Kharagpur, India.

Author Contributions: J. S., R. V. K. and M. B. designed the research project, J. S. and M. C. performed

numerical simulations, J. S. and M. B. performed analytical calculations, J. S., C. P. J. A. and M. B. contributed to MA concepts, M. C. contributed to VED concepts, J. S., R. V. K. and M. B. interpreted results, all authors contributed to writing of the manuscript.

Competing financial interests: The authors declare no competing financial interests.

-
- [1] Greiner, M., Mandel, O., Esslinger, T., Hänsch, T.W., & Bloch, I. Quantum phase transition from a superfluid to a Mott insulator in a gas of ultracold atoms. *Nature* **415**, 39-44 (2002).
 - [2] Joyce, G.S. Absence of ferromagnetism or antiferromagnetism in the isotropic Heisenberg model with long-range interactions. *Journal of Physics C: Solid State Physics*, **2**, 1531-1533 (1969).
 - [3] Bruno, P. Absence of spontaneous magnetic order at nonzero temperature in one- and two-dimensional Heisenberg and XY systems with long-range Interactions. *Phys. Rev. Lett.* **87**, 137203 (2001).
 - [4] Doniach, S. & Inui, M. Long-range Coulomb interactions and the onset of superconductivity in the high- T_c materials. *Phys. Rev. B* **41**, 6668-6678 (1990).
 - [5] Soltan-Panahi, P., Lühmann, D.-S., Struck J., Windpassinger, W. & Sengstock, K. Quantum phase transition to unconventional multi-orbital superfluidity in optical lattices. *Nat. Phys.* **8**, 71-75 (2012).
 - [6] Pollet, L., Picon, J.D., Büchler, H.P. & Troyer, M. Supersolid phase with cold polar molecules on a triangular Lattice. *Phys. Rev. Lett.* **104**, 125302 (2010).
 - [7] Landau, L.D. Über die bewegung der elektronen in kristallgitter. *Phys. Z. Sowjetunion* **3**, 644-645 (1933).
 - [8] Feynman, R.P. Slow electrons in a polar Crystal. *Phys. Rev.* **97**, 660-665 (1955).
 - [9] Feynman, R.P., Hellwarth, R.W., Iddings, C.K. & Platzman, P.M. Mobility of slow electrons in a polar crystal. *Phys. Rev.* **127**, 1004-1017 (1962).
 - [10] Galitskii, V.M. & Migdal, A.B. Application of quantum field theory methods to the many body problem. *JETP* **34**, 139-150 (1958).
 - [11] Engelsberg, S. & Schrieffer, J.R. Coupled electron-phonon system. *Phys. Rev.* **131**, 993-1008 (1963).
 - [12] Tyablikov, S.V. On electron energy spectrum in polar crystal. *Zh. Eksp. Teor. Fiz.* **23**, 381 (1952).
 - [13] Holstein, T. Studies of polaron motion: Part II. The "small" polaron. *Annals of Physics* **8**, 343-389 (1959).
 - [14] Fröhlich, H., Pelzer & H., Zienau, S. Properties of slow electrons in polar materials. *Philos. Mag.* **41**, 221-242 (1954).
 - [15] Fröhlich, H. Electrons in lattice fields. *Adv. Phys.* **3**, 325-361 (1954).
 - [16] Barišić, S., Labbé, J. & Friedel, J. Tight binding and transition-metal superconductivity. *Phys. Rev. Lett.* **25**, 919-922 (1972).
 - [17] Barišić, S., Rigid-atom electron-phonon coupling in the tight-binding approximation. I. *Phys. Rev. B* **5**, 932-94 (1972).
 - [18] Barišić, S., Self-consistent electron-phonon coupling in the tight-binding approximation. II. *Phys. Rev. B* **5**, 941-951 (1972).
 - [19] Su, W.P., Schrieffer, J.R. & Heeger, A.J. Solitons in Polyacetylene. *Phys. Rev. Lett.* **42**, 1698-1701 (1979).
 - [20] Heeger, A.J., Kivelson, S., Schrieffer, J.R. & Su, W.P. Solitons in conducting polymers. *Rev. Mod. Phys.* **60**, 781-850 (1988).
 - [21] Marchand, D.J.J. et al. Sharp transition for single polarons in the one-dimensional Su-Schrieffer-Heeger model. *Phys. Rev. Lett.* **105**, 266605 (2010).
 - [22] Edwards, D.M. A quantum phase transition in a model with boson-controlled hopping. *Physica B* **378**, 133-134 (2006).
 - [23] Alvermann, A., Edwards, D.M., & Fehske, H. Boson-controlled quantum transport. *Phys. Rev. Lett.* **98**, 056602 (2007).
 - [24] Berciu, M. & Fehske, H. Momentum average approximation for models with boson-modulated hopping: Role of closed loops in the dynamical generation of a finite quasiparticle mass. *Phys. Rev. B* **82**, 085116 (2010).
 - [25] Chakraborty, M., Mohanta, N., Taraphder, A., Min, B.I. & Fehske, H. Edwards polaron formation : From one to three dimensions. *Phys. Rev. B* **93**, 155130 (2016).
 - [26] Trugman, S.A. Interaction of holes in a Hubbard antiferromagnet and high-temperature superconductivity. *Phys. Rev. B* **37**, 1597-1603 (1988).
 - [27] Pearson, C.J., Barford, W. & Bursill, R.J. Quantized lattice dynamic effects on the Peierls transition of the extended Hubbard-Peierls model. *Phys. Rev. B* **83**, 195105 (2011).
 - [28] Scholes, G.D. & Rumbles, G. Excitons in nanoscale systems. *Nat. Mater.* **5**, 683-696 (2006).
 - [29] Park, S.H. et al. Bulk heterojunction solar cells with internal quantum efficiency approaching 100 %. *Nat. Photon.* **3**, 297-302 (2009).
 - [30] Hauke, P. et al. Complete devil's staircase and crystal-superfluid transitions in a dipolar XXZ spin chain: A trapped ion quantum simulation. *New J. Phys.* **12**, 113037 (2010).
 - [31] Stojanović, V.M., Shi, T., Bruder, C. & Cirac, J.I. Quantum simulation of small-polaron Formation with trapped Ions. *Phys. Rev. Lett.* **109**, 250501 (2012).
 - [32] Bermudez, A., Schaetz, T. & Plenio, M.B. Dissipation-assisted quantum information processing with trapped ions. *Phys. Rev. Lett.* **110**, 110502 (2013).
 - [33] Bermudez, A. & Schaetz, T. Quantum transport of energy in controlled synthetic quantum magnets. *New J. Phys.* **18**, 083006 (2016).
 - [34] Mülken, O. et al. Survival probabilities in coherent exciton transfer with trapping. *Phys. Rev. Lett.* **99**, 090601 (2007).
 - [35] Ates, C., Eisfeld, A. & Rost, J.M. Motion of Rydberg

- atoms induced by resonant dipole-dipole interactions. *New J. Phys.* **10**, 045030 (2008).
- [36] Hague, J.P. & MacCormick, C. Quantum simulation of electron-phonon interactions in strongly deformable materials. *New J. Phys.* **14**, 033019 (2012).
- [37] Hague, J.P. & MacCormick, C. Bilayers of Rydberg atoms as a quantum simulator for unconventional superconductors. *Phys. Rev. Lett.* **109**, 223001 (2012).
- [38] Günter, G. et al. Observing the dynamics of dipole-mediated energy transport by interaction-enhanced Imaging. *Science* **342**, 954-956 (2013).
- [39] Rabl, P. & Zoller, P. Molecular dipolar crystals as high-fidelity quantum memory for hybrid quantum computing. *Phys. Rev. A* **76**, 042308 (2007).
- [40] Ortner, M., Micheli, A., Pupillo, G. & Zoller, P. Quantum simulations of extended Hubbard models with dipolar crystals. *New J. Phys.* **11**, 055045 (2009).
- [41] Zhou, Y.L., Ortner, M. & Rabl, P. Long-range and frustrated spin-spin interactions in crystals of cold polar molecules. *Phys. Rev. A* **84**, 052332 (2011).
- [42] Herrera, F. & Krems, R.V. Tunable Holstein model with cold polar molecules. *Phys. Rev. A* **84**, 051401(R) (2011).
- [43] Herrera, F., Madison, K.W., Krems, R.V. & Berciu, M. Investigating polaron transitions with polar molecules. *Phys. Rev. Lett.* **110**, 223002 (2013).
- [44] Mostame, S. et al. Quantum simulator of an open quantum system using superconducting qubits: Exciton transport in photosynthetic complexes. *New J. Phys.* **14**, 105013 (2012).
- [45] Agarwal, K., Martin, I., Lukin, M.D. & Demler, E. Polaronic model of two-level systems in amorphous solids. *Phys. Rev. B* **87**, 144201 (2013).
- [46] Mei, F., Stojanović, V.M., Siddiqi, I. & Tian, L. Analog superconducting quantum simulator for Holstein polarons. *Phys. Rev. B* **88**, 224502 (2013).
- [47] Stojanović, V.M., Vanević, M., Demler, E. & Tian, L. Transmon-based simulator of nonlocal electron-phonon coupling: A platform for observing sharp small-polaron transitions. *Phys. Rev. B* **89**, 144508 (2014).
- [48] Lanting, T. et al. Entanglement in a quantum annealing processor. *Phys. Rev. X* **4**, 021041 (2014).
- [49] Huh, J., Mostame, S., Fujita, T., Yung, M.-H. & Aspuru-Guzik, A. Linear-algebraic bath transformation for simulating complex open quantum systems. *New J. Phys.* **16**, 123008 (2014).
- [50] Spano, F.C. The Spectral signatures of Frenkel polarons in H- and J-aggregates. *Acc. Chem. Res.*, **43**, 429-439 (2010).
- [51] Schirotzek, A., Wu, C.-H., Sommer, A. & Zwierlein, M.W. Observation of Fermi polarons in a tunable Fermi liquid of ultracold Atoms. *Phys. Rev. Lett.* **102**, 230402 (2008).
- [52] Massignan, P., Zaccanti & M., Bruun, G.M. Polarons, dressed molecules and itinerant ferromagnetism in ultracold Fermi gases. *Rep. Prog. Phys.* **77**, 034401 (2014).
- [53] Cetina, M. et al. Ultrafast many-body interferometry of impurities coupled to a Fermi sea. *Science* **354**, 96-99 (2016).
- [54] Klein, A., Bruderer, M., Clark, S.R. & Jaksch, D. Dynamics, dephasing and clustering of impurity atoms in Bose-Einstein condensates. *New J. Phys.* **9**, 411 (2007).
- [55] Catani, J. et al. Quantum dynamics of impurities in a one-dimensional Bose gas. *Phys. Rev. A* **85**, 023623 (2012).
- [56] Spethmann, N. et al. Dynamics of single neutral impurity atoms immersed in an ultracold gas. *Phys. Rev. Lett.* **109**, 235301 (2012).
- [57] Casteels, W., Tempere, J. & Devreese, J.T. Bipolarons and multipolarons consisting of impurity atoms in a Bose-Einstein condensate. *Phys. Rev. A* **88**, 013613 (2013).
- [58] Shashi, A., Grusdt, F., Abanin, D.A. & Demler, E. Radio-frequency spectroscopy of polarons in ultracold Bose gases. *Phys. Rev. A* **89**, 053617 (2014).
- [59] Hohmann, M. et al. Neutral impurities in a Bose-Einstein condensate for simulation of the Fröhlich-polaron. *EPJ Quant. Tech.* **2**, 23 (2015).
- [60] Nie, W., Katsura, H. & Oshikawa, M. Ground-State Energies of Spinless Free Fermions and Hard-Core Bosons. *Phys. Rev. Lett.* **111**, 100402 (2013).
- [61] Greiter, M., Schnells, V. & Thomale, R. The 1D Ising model and the topological phase of the Kitaev chain. *Annals of Physics* **351**, 1026-1033 (2014).
- [62] Bonča, J., Katrašnik, T. & Trugman, S.A. Mobile bipolaron. *Phys. Rev. Lett.* **84**, 3153-3156 (2000).
- [63] Bonča, J. & Trugman, S.A. Bipolarons in the extended Holstein Hubbard model. *Phys. Rev. B* **64**, 094507 (2001).
- [64] Chakraborty, M., Min, B.I., Chakrabarti, A. & Das, A.N. Stability of Holstein and Fröhlich bipolarons. *Phys. Rev. B* **85**, 245127 (2012).
- [65] Berciu, M. Green's function of a dressed particle. *Phys. Rev. Lett.* **97**, 036402 (2006).
- [66] Berciu, M. & Goodvin, G.L. Systematic improvement of the momentum average approximation for the Green's function of a Holstein polaron. *Phys. Rev. B* **76**, 165109 (2007).
- [67] Goodvin, G.L. & Berciu, M. Momentum average approximation for models with electron-phonon coupling dependent on the phonon momentum. *Phys. Rev. B* **78**, 235120 (2008).
- [68] Hague, J.P. & Kornolovitch, P.E. Bipolarons from long-range interactions: Singlet and triplet pairs in the screened Hubbard-Fröhlich model on the chain. *Phys. Rev. B* **80**, 054301 (2009).
- [69] Berciu, M. Few-particle Green's functions for strongly correlated systems on infinite lattices. *Phys. Rev. Lett.* **107**, 246403 (2011).

Supplementary Material for
“Phonon-mediated repulsion, sharp transitions and
(quasi)self-trapping in the extended Peierls-Hubbard model”

J. Sous, M. Chakraborty, C. P. J. Adolphs, R. V. Krems, and M. Berciu

(Dated: January 3, 2018)

MOMENTUM AVERAGE (MA) APPROXIMATION - TECHNICAL DETAILS

The Momentum Average (MA) [1–3] approximation is a non-perturbative quasi-analytical technique designed to solve the equation of motion for the relevant Green’s function $G(k, \omega) = \langle k | (\omega - \mathcal{H} + i\eta)^{-1} | k \rangle$ in the Bogoliubov-Born-Green-Kirkwood-Yvon (BBKGY) hierarchy. The hierarchy consists of an infinite set of coupled equations which are impossible to solve exactly. By neglecting exponentially small contributions in the expansion, one simplifies the equations of motion to a form that is readily solvable numerically. The guide to approximating the hierarchy follows from the variational meaning of MA: essentially one solves the problem in a variational subspace.

The choice of the variational space depends on the details of the Hamiltonian and state(s) of interest [2]. For the Holstein model, a one-site phonon cloud suffices to provides accurate results for single polarons [1, 2] and for S0 bipolarons [5]. S0 bipolarons are single-site strongly bound bipolarons. Taken together with the local nature of the Holstein coupling, this explains why a one-site phonon cloud is accurate to describe such states. For the Edwards and SSH models, the coupling to phonons is non-local and therefore a bigger cloud is required to yield accurate results. A three-site phonon cloud MA has been shown to be very accurate for such models [4, 6].

In this work, we generalize MA to study strongly bound two-particle states in the extended Peierls/Su-Schrieffer-Heeger (SSH)–Hubbard model. We derive the MA equations for two hardcore particles in a three-site phonon cloud and allow the particles to be arbitrarily far from the cloud but at most two sites apart from each other, if a cloud is present. Terms corresponding to the particles being further than two sites apart are expected to contribute significantly only to higher-energy states, if a two-particle state is strongly bound, which is the case of primary interest to us in this work. For weakly bound dimers, the variational space must be extended to include configurations where the particles are further apart. The variational space can be increased systematically until convergence is achieved.

To highlight the method we derive a few representative equations of motion used in the MA formalism developed here [7]. This is achieved using Dyson’s identity $\hat{G}(\omega) = \hat{G}_0(\omega) + \hat{G}(\omega)\hat{V}\hat{G}_0(\omega)$ where $\hat{G}(\omega) = (\omega - \mathcal{H} + i\eta)^{-1}$, $\hat{G}_0(\omega) = (\omega - \mathcal{H}_0 + i\eta)^{-1}$ with $\mathcal{H}_0 = \mathcal{H}_p + \mathcal{H}_{ph}$, and \hat{V} is the bare particle - phonon coupling term.

Consider the two-particle propagator $G(K, 1, n, \omega) = \langle K, 1 | \hat{G}(\omega) | K, n \rangle$ defined for two-

particle states $|K, n\rangle = \sum_i \frac{e^{iK(R_i + na/2)}}{\sqrt{N}} c_i^\dagger c_{i+n}^\dagger |0\rangle$ with the two particles $n \geq 1$ sites apart, and a is the lattice constant. Using Dyson's identity and inserting a resolution of the identity, its exact equation of motion can be written as:

$$G(K, 1, n, \omega) = G_0(K, 1, n, \omega) + \sum_{\eta} G_0(K, \eta, n, \omega) \langle K, 1 | \hat{G}(\omega) \hat{V} | K, \eta \rangle.$$

Note that $G_0(K, 1, n, \omega)$ can be calculated exactly analytically in one dimension [8]. Consider now $\hat{V} | K, \eta \rangle$. It consists of states with one phonon plus the particles $\eta \pm 1$ sites apart. Thus, the right-hand side of the exact equation of motion contains an infinite number of terms. Because within MA we restrict the particles to be within two sites of each other when phonons are present, this simplifies the equation of motion to:

$$\begin{aligned} G(K, 1, n, \omega) = & G_0(K, 1, n, \omega) \\ & - g e^{-iKa} G_0(K, 2, n, \omega) F_1(-2, 1) + g G_0(K, 2, n, \omega) F_1(-1, 1) \\ & - g G_0(K, 2, n, \omega) F_1(0, 1) + g e^{iKa} G_0(K, 2, n, \omega) F_1(1, 1) \\ & - g e^{-3iKa/2} G_0(K, 3, n, \omega) F_1(-3, 2) \\ & - g [e^{-3iKa/2} G_0(K, 1, n, \omega) - e^{-iKa/2} G_0(K, 3, n, \omega)] F_1(-2, 2) \\ & - 2ig \sin(Ka/2) G_0(K, 1, n, \omega) F_1(-1, 2) \\ & + g [e^{3iKa/2} G_0(K, 1, n, \omega) - e^{iKa/2} G_0(K, 3, n, \omega)] F_1(0, 2) \\ & + g e^{3iKa/2} G_0(K, 3, n, \omega) F_1(1, 2), \end{aligned} \quad (1)$$

where $F_1(m, n)$ is shorthand for $F_1(K, m, n, \omega)$ defined as

$$F_l(K, m, n, \omega) \equiv \sum_i \frac{e^{iKR_i}}{\sqrt{N}} \langle K, 1 | \hat{G}(\omega) c_{i+m}^\dagger c_{i+m+n}^\dagger b_i^{\dagger l_1} b_{i+1}^{\dagger l_2} | 0 \rangle, \quad (2)$$

i.e. a generalized one-site cloud propagator. By introducing other appropriate generalized propagators:

$$F_{l_1, l_2}(K, m, n, \omega) \equiv \sum_i \frac{e^{iKR_i}}{\sqrt{N}} \langle K, 1 | \hat{G}(\omega) c_{i+m}^\dagger c_{i+m+n}^\dagger b_i^{\dagger l_1} b_{i+1}^{\dagger l_2} | 0 \rangle, \quad (3)$$

$$F_{l_1, l_2, l_3}(K, m, n, \omega) \equiv \sum_i \frac{e^{iKR_i}}{\sqrt{N}} \langle K, 1 | \hat{G}(\omega) c_{i+m}^\dagger c_{i+m+n}^\dagger b_{i-1}^{\dagger l_1} b_i^{\dagger l_2} b_{i+1}^{\dagger l_3} | 0 \rangle, \quad (4)$$

for two-site cloud and three-site cloud configurations respectively, and repeatedly applying the Dyson's identity, one derives the MA equations of motion for the the propagators in Eqs.

(1)-(4). This linear system of coupled equations is solved numerically and the propagator of interest $G(K, 1, n, \omega)$ is computed. Dimer bound state properties such as $E_D(K)$ can be extracted from the propagator.

By construction the MA approach developed here is designed to describe strongly bound states accurately. Indeed, the comparison with Variational Exact Diagonalization (VED) results shows that the MA approximation is accurate in this regime. By systematically extending the variational subspace we expect to be able to study weakly-bound dimers as well.

PERTURBATION THEORY (PT) RESULTS IN THE LIMIT $\Omega \gg |t|, |g|$

Single-particle sector

Let \hat{P} be the projector onto the zero-phonon Hilbert subspace, which is spanned by the states $c_i^\dagger|0\rangle, \forall i$. The effective Hamiltonian in this subspace is, to second order in perturbation theory:

$$\hat{h}_1 = \hat{T} + \hat{P}\hat{V}\frac{1}{E_0 - \mathcal{H}_0}\hat{V}\hat{P},$$

where $\hat{T} = -t\sum_i(c_i^\dagger c_{i+1} + h.c.)$ is the bare kinetic energy, \hat{V} is the bare particle - phonon coupling from Eq. (1) in the main text, and $\mathcal{H}_0 = \mathcal{H}_{\text{ph}}$. The projection is straightforward to carry out and leads to:

$$\hat{h}_1 = \hat{T} + \hat{T}_2 - \frac{4g^2}{\Omega}\sum_i \hat{n}_i, \quad (5)$$

where $\hat{T}_2 = +t_2\sum_i(c_i^\dagger c_{i+2} + h.c.)$ is a phonon-mediated next-nearest-neighbor (NNN) hopping with $t_2 = g^2/\Omega = \lambda t/2$ (note the unusual sign). For convenience we define $\epsilon_0 = \frac{4g^2}{\Omega}$.

Setting $a = 1$, the polaron dispersion is, therefore,

$$E_P(k) = -\epsilon_0 - 2t \cos(k) + 2t_2 \cos(2k).$$

It is straightforward to verify that if $t > 4t_2$, *i.e.* if $\lambda < \frac{1}{2}$, the polaron ground state (GS) momentum is 0. For $\lambda > \frac{1}{2}$, the polaron GS momentum is $k_P = \arccos \frac{t}{4t_2}$, going asymptotically to $\frac{\pi}{2}$ as $\lambda \rightarrow \infty$.

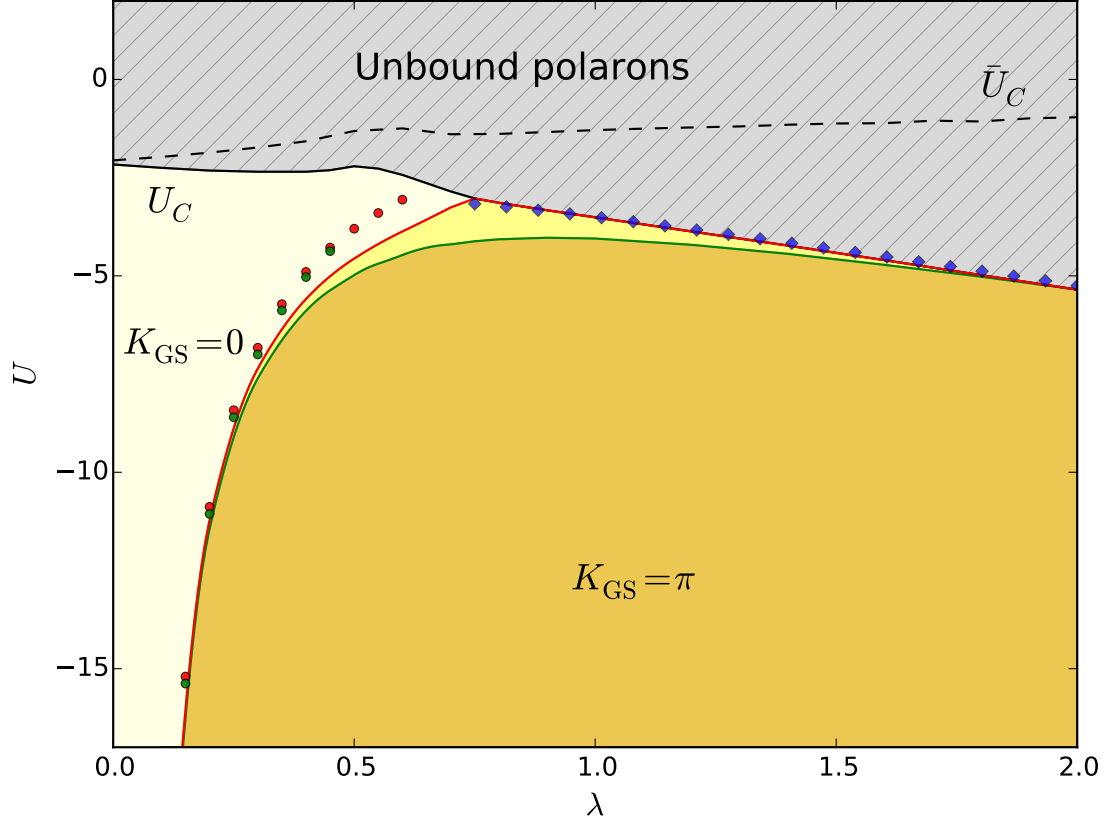


FIG. 1. (color online) Two-polaron phase diagram for $t = 1$, $\Omega = 100$. The solid black line shows $U_C(\lambda)$ below which stable bound states form, while the dashed line shows $\bar{U}_C(\lambda)$ defined in the main text; the difference between the two is the strength of the phonon-mediated repulsion. The red and green lines mark the sharp transitions of the bound dimer's GS. The lines are the VED results and the symbols of the corresponding color are the MA results. The diamond symbols are the PT results of Eq. (7). The area between the red and green curves corresponds to a dimer bound state with $0 < K_{\text{GS}} < \pi$.

Two-particle sector

Repeating the projection onto the two-bare particle – zero-phonon subspace spanned by the states $c_i^\dagger c_{i+n}^\dagger |0\rangle$, $\forall n \geq 1, i$, we find:

$$\hat{h}_2 = \hat{T} + \hat{T}_2 - \epsilon_0 \sum_i \hat{n}_i + \tilde{U} \sum_i \hat{n}_i \hat{n}_{i+1}, \quad (6)$$

where $\tilde{U} = U + \epsilon_0$; U is the bare nearest-neighbor (NN) interaction.

The two-polaron bound state dispersion can be calculated numerically, either using direct diagonalization for a large-enough chain, or using the Equation-of-Motion (EOM) approach. We briefly present the latter and then use it to obtain analytical solutions in some specific limits.

We define $|K, n\rangle = \sum_i \frac{e^{iK(R_i + \frac{n}{2})}}{\sqrt{N}} c_i^\dagger c_{i+n}^\dagger |0\rangle$, $\forall n \geq 1$, and the propagators $g(n) \equiv \langle K, 1 | \hat{G}(\omega) | K, n \rangle$, where $\hat{G}(\omega) = (\omega + i\eta - \hat{h}_2)^{-1}$ is the resolvent of interest. The bound state energy (once a bound state appears) is at the lowest discrete pole of these propagators. Using the identity $\hat{G}(\omega)(\omega + i\eta - \hat{h}_2)^{-1} = 1$, we generate the EOM:

$$\begin{aligned} (\omega + i\eta - \tilde{U} + 2\epsilon_0 - \beta_K)g(1) &= 1 - \alpha_K g(2) + \beta_K g(3) \\ (\omega + i\eta + 2\epsilon_0)g(2) &= -\alpha_K [g(1) + g(3)] + \beta_K g(4) \end{aligned}$$

and for any $n \geq 3$,

$$\begin{aligned} (\omega + i\eta + 2\epsilon_0)g(n) &= -\alpha_K [g(n-1) + g(n+1)] \\ &\quad + \beta_K [g(n-2) + g(n+2)]. \end{aligned}$$

Here, $\alpha_K = 2t \cos(\frac{K}{2})$, $\beta_K = 2t_2 \cos(K)$.

The physically acceptable analytical solution for recurrence relations of this type is available in [9], however it is rather complicated and its poles cannot be extracted analytically. A general solution can be found numerically.

There are two cases that can be solved rather easily analytically, namely (i) if $\beta_K = 0$, and (ii) if $\alpha_K = 0$. The first is realized when $t_2 = 0$, and can be used as an indication of physics at very weak couplings $\lambda \rightarrow 0$. In this case the recurrence relation becomes trivial. For any $n \geq 2$ we have $g(n) = z(K, \omega)g(n-1)$ where

$$z(K, \omega) = \frac{1}{2\alpha_K} \left[-\tilde{\omega} + \sqrt{\tilde{\omega} + 2\alpha_K} \sqrt{\tilde{\omega} - 2\alpha_K} \right]$$

and $\tilde{\omega} \equiv (\omega + i\eta + 2\epsilon_0)$. This results in:

$$g(K, n, \omega) = 2 \frac{[z(K, \omega)]^{n-1}}{\tilde{\omega} - 2\tilde{U} + \sqrt{\tilde{\omega} + 2\alpha_K} \sqrt{\tilde{\omega} - 2\alpha_K}}$$

for which exists a line cut that indicates a continuum (the two-particle continuum) for $|\tilde{\omega}| \leq 2\alpha_K$. A bound dimer appears if and only if there is a discrete pole at $\omega = E_D(K)$ such that a) $E_D(K) + 2\epsilon_0 < -2\alpha_K$ (the pole is below the continuum) and b) $E_D(K) + 2\epsilon_0 -$

$2\tilde{U} + \sqrt{E_D(K) + 2\epsilon_0 + 2\alpha_K} \sqrt{E_D(K) + 2\epsilon_0 - 2\alpha_K} = 0$ (the pole condition). It follows that the solution is

$$E_D(K) = -2\epsilon_0 + \tilde{U} + \frac{\alpha_K^2}{\tilde{U}},$$

which is below the continuum if and only if $\tilde{U} \leq -\alpha_K$. In particular, this requires $\tilde{U} < -2t$ for a bound state to emerge in the entire Brillouin zone, even at $K = 0$. This finite bare NN attraction is necessary in order to compensate for the lost kinetic energy, when the two particles bind.

The second accessible analytical solution is for $\alpha_K = 0$, which is valid for $K = \pi$ irrespective of the value of t , and therefore will give the exact PT bound dimer solution at the edge of the Brillouin zone. The solution follows as before, and it results in:

$$g(K, 1, \omega) = \frac{2}{\tilde{\omega} - 2\tilde{U} + 4t_2 + \sqrt{\tilde{\omega} - 4t_2}\sqrt{\tilde{\omega} + 4t_2}}$$

for which, repeating the analysis, we find that a discrete bound state appears if and only if $\tilde{U} < 0 \rightarrow U < -2\lambda t$, and its energy is $E_D(\pi) = -2\epsilon_0 + \tilde{U} - 2t_2 + \frac{4t_2^2}{\tilde{U} - 2t_2}$.

Note that the definition we employ for a *stable* bound state is not one that lies below the continuum at its momentum, but one that lies below the edge (lowest overall possible value) of the continuum. If this more stringent condition is not met, coupling to other fields (acoustic phonons, photons, ...) would allow transitions from this discrete state into the bottom of the continuum, so the dimer state is not truly stable.

To calculate U_C according to this definition, we compute the lower edge of the continuum. Given the single polaron dispersion $E_P(k)$ (calculated in the previous section), and noting that at a given total momentum K the two-polaron continuum start at $\min_q[E_P(K - q) + E_P(q)]$, one can easily solve for the lower edge of the continuum, E_c . One finds the result $E_c = 2 \min_k E_P(k)$, *i.e.* twice the polaron GS energy.

Requiring that $E_D(\pi) < E_c$ leads to

$$U_C(\lambda) = -2\lambda t - t - \frac{t}{2\lambda} + \mathcal{O}\left(\frac{1}{\lambda^2}\right). \quad (7)$$

This should agree with numerical results for sufficiently large λ where the GS momentum of the bound state approaches $K_{GS} = \pi$. However, note that λ should still be small enough such that PT remains valid. For example, for $\Omega = 100, t = 1$ this would require $\lambda < 2 \rightarrow g < 10$ such that $g/\Omega \ll 1$. For stronger couplings one needs to go to higher order(s) in perturbation theory.

Indeed, Fig. 1 shows good agreement at moderate and large $\lambda \leq 2$ between $U_C(\lambda)$ and this analytical prediction of Eq. (7).

-
- [1] Berciu, M. Green's function of a dressed particle. *Phys. Rev. Lett.* **97**, 036402 (2006).
 - [2] Berciu, M. & Goodvin, G.L. Systematic improvement of the momentum average approximation for the Green's function of a Holstein polaron. *Phys. Rev. B* **76**, 165109 (2007).
 - [3] Goodvin, G.L. & Berciu, M. Momentum average approximation for models with electron-phonon coupling dependent on the phonon momentum. *Phys. Rev. B* **78**, 235120 (2008).
 - [4] Marchand, D.J.J. et al. Sharp transition for single polarons in the one-dimensional Su-Schrieffer-Heeger model. *Phys. Rev. Lett.* **105**, 266605 (2010).
 - [5] Adolphs, C.P.J. & Berciu, M. Strongly bound yet light bipolarons for double-well electron-phonon coupling. *Phys. Rev. B* **90**, 085149 (2014).
 - [6] Berciu, M. & Fehske, H. Momentum average approximation for models with boson-modulated hopping: Role of closed loops in the dynamical generation of a finite quasiparticle mass. *Phys. Rev. B* **82**, 085116 (2010).
 - [7] Sous, J. et al., in preparation.
 - [8] Berciu, M. Few-particle Green's functions for strongly correlated systems on infinite lattices. *Phys. Rev. Lett.* **107**, 246403 (2011).
 - [9] Möller, M., Mukherjee, A., Adolphs, C.P.J., Marchand, D.J.J. & Berciu, M. Efficient computation of lattice Green functions for models with longer range hopping. *J. Phys. A: Math. Theor.* **45**, 115206 (2012).